Electronic supplementary materials

For https://doi.org/10.1631/jzus.A2500436

Numerical investigation of the flow pattern around a vertical cylinder under wave action

Ben HE[1], Junkang WENG[2], Yuan LIN[2], Yifan GAO[1], Maoxing WEI[2], Fang HE[2]✉

[1]*PowerChina Huadong Engineering Co., Ltd., Hangzhou 311100, China*
[2]*Ocean College, Zhejiang University, Zhoushan 316021, China*

✉ Fang HE, hefang@zju.edu.cn

Section S1 Comparison of numerical results with PIV results

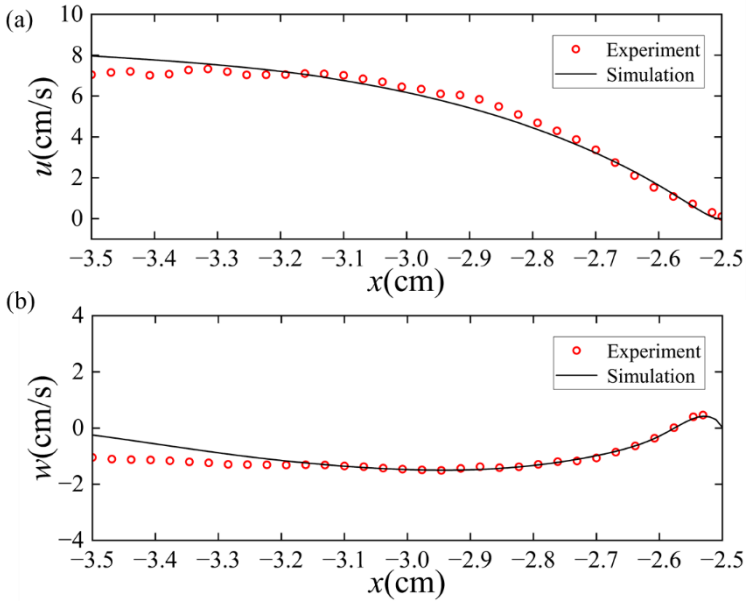

Fig. S1 Comparison of velocity profiles at *z*=0.6cm between the PIV and simulation. (a) horizontal velocity verification; (b) vertical velocity verification

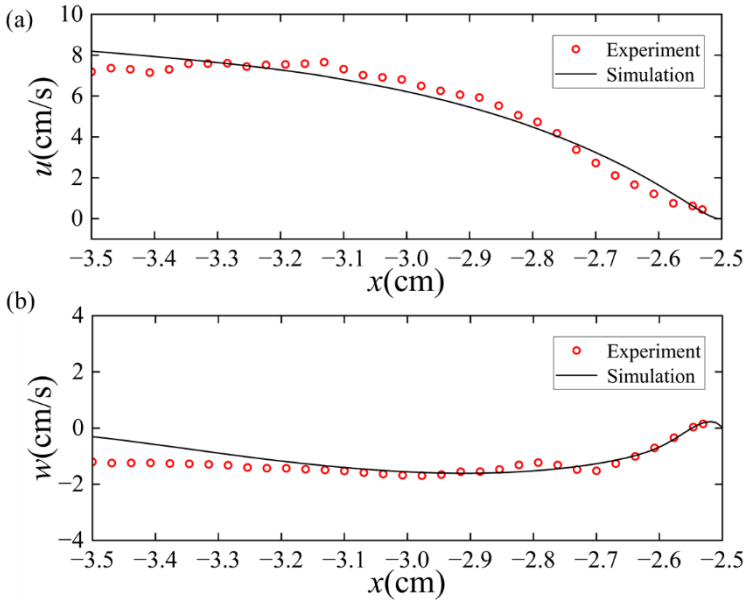

Fig. S2 Comparison of velocity profiles at z=0.8cm between the PIV and simulation. (a) horizontal velocity verification; (b) vertical velocity verification

Section S2 Discussion of streamlines and velocity distributions in the wake of the cylinder

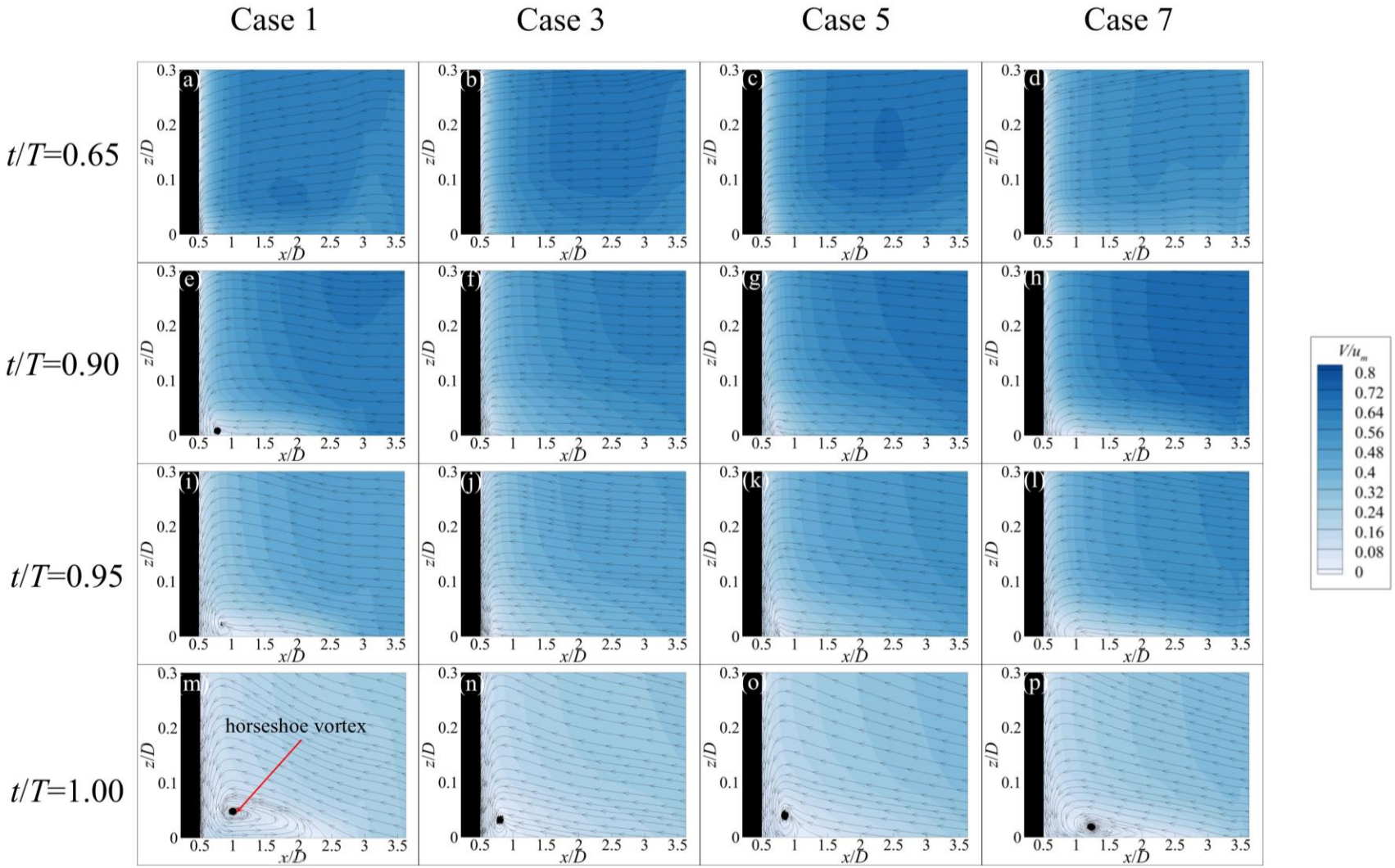

Fig. S3 Streamlines and velocity distribution behind the cylinder. (a) Case 1 at *t*/*T*=0.65; (b) Case 3 at *t*/*T*=0.65; (c) Case 5 at *t*/*T*=0.65; (d) Case 7 at *t*/*T*=0.65; (e) Case 1 at *t*/*T*=0.90; (f) Case 3 at *t*/*T*=0.90; (g) Case 5 at *t*/*T*=0.90; (h) Case 7 at *t*/*T*=0.90; (i) Case 1 at *t*/*T*=0.95; (j) Case 3 at *t*/*T*=0.95; (k) Case 5 at *t*/*T*=0.95; (l) Case 7 at *t*/*T*=0.95; (m) Case 1 at *t*/*T*=1.00; (n) Case 3 at *t*/*T*=1.00; (o) Case 5 at *t*/*T*=1.00; (p) Case 7 at *t*/*T*=1.00

Fig. S3 presents streamlines and velocity distributions in the wake of the cylinder for the selected cases. The downstream flow exhibits significant structural differences compared to the upstream region (as shown in Fig. 3). Specifically, the horseshoe vortex exhibits spatial contraction in the downstream region, as can be seen from Figs. S3(e) and S3(i). Notably, in contrast to the complex vortex interactions observed upstream, no coexistence of double vortices is observed downstream. In all four selected cases, horseshoe vortices are generated near the cylinder, with their vortex cores confined within the ranges $0.5<x/D<1.5$ and $0<z/D<0.05$. This suggests that, although the flow conditions vary under different *KC* numbers, the vortex formation mechanism retains an inherent regularity. As shown in Figs. S3(m), S3(n), B(o), and S3(p), at lower *KC* numbers, the spiral streamlines remain tightly constrained around the vortex cores. With increasing *KC*, the area occupied by the curved spiral streamlines progressively expands, reflecting an intensified influence of the horseshoe vortex on the overall flow field. However, despite the increased vortex activity, the fundamental morphological stability of the downstream flow is maintained.

Section S3 Partial enlarged image of *Q* criterion contour

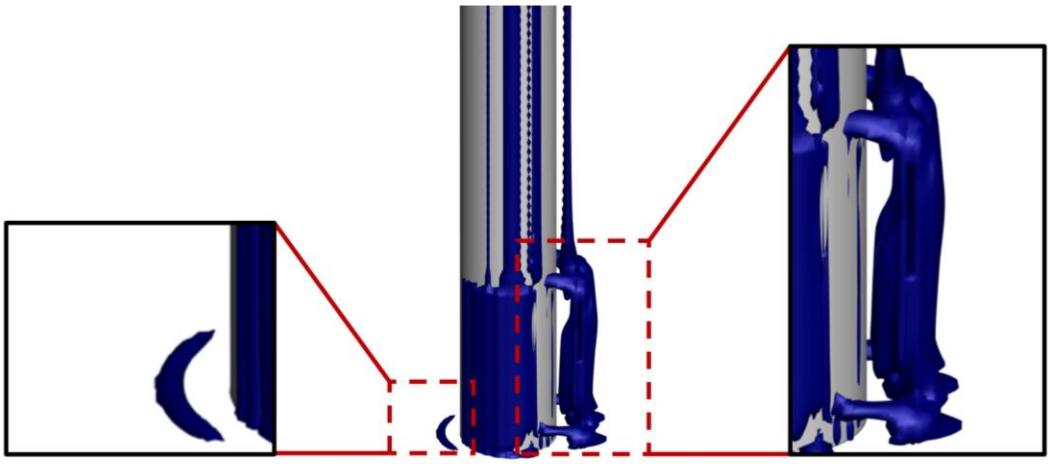

Fig. S4 Case 1 *t*/*T*=0.39

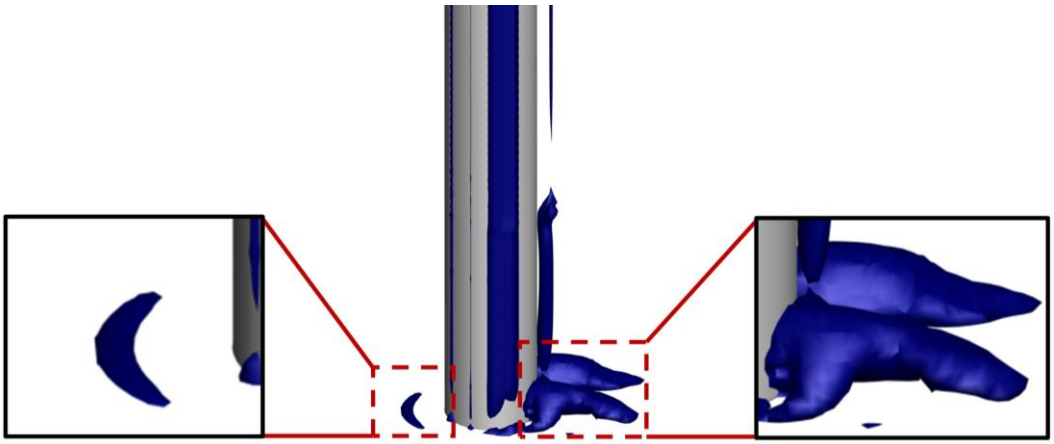

Fig. S5 Case 7 *t*/*T*=0.30